

The Ter-Mikayelian Effect on QCD Radiative Energy Loss

Magdalena Djordjevic and Miklos Gyulassy

*Dept. Physics, Columbia University, 538 W 120-th Street,
New York, NY 10027, USA*

July 16, 2003

Abstract

The color dielectric modification of the gluon dispersion relation in a dense QCD medium suppresses both the soft and collinear gluon radiation associated with jet production. We compute the longitudinal and transverse plasmon contributions to the zeroth order in opacity radiative energy loss in the 1-loop HTL approximation. This is QCD analog of the Ter-Mikayelian effect in QED and leads to $\sim 30\%$ reduction of the energy loss of high transverse momentum charm quarks produced in a QCD plasma with a characteristic Debye mass $\mu \sim 0.5$ GeV.

1 Introduction

Jet tomography in ultra-relativistic nuclear collisions can be used to map out the density of the produced QCD plasma from the suppression pattern of high transverse momentum hadrons [1]-[9]. The quenching of jets [10, 11] is mainly due to the medium induced radiative energy loss of high energy partons propagating through ultra-dense QCD matter. However, even if final state multiple elastic and inelastic interactions are neglected, gluon radiation associated with hard QCD processes already softens considerably the lowest order jet spectra. In elementary particle collisions, this *associated* radiation can be taken into account through the Q^2 (DGLAP) evolution of the hadronic fragmentation functions. In a plasma, even the associated radiation is modified by the dielectric properties of that medium as first pointed out by Ter-Mikayelian [12, 13]. The non-abelian QCD analog of the Ter-Mikayelian plasmon effect is the subject of this paper. A summary of our main results has been published in paper I[14]. In this paper, the details of Ter-Mikayelian calculations are presented.

This work is motivated by the surprising observation of PHENIX [15] that “prompt” single electron spectrum from open charm production in $Au + Au$ collisions at $\sqrt{s} = 130$ AGeV shows no sign of heavy quark energy loss [16]. In contrast, a dramatic suppression (by a factor ~ 5) was observed at RHIC for pions with $p_T > 3$ GeV originating from the fragmentation of light quark and gluons [17]-[25]. See a recent reviews of light quark and gluon tomography in A+A in [26]-[27]. The suppression of light hadrons is consistent with the expected large radiative induced energy loss of light quark and gluon jets in an ultra-dense plasma of density approximately 100 times higher than in ground state nuclei [2].

The spectrum of induced radiation depends on the optical thickness or opacity $\chi = L/\lambda$ of the plasma, and has been computed to arbitrary order in χ^n for massless partons in GLV [4, 26]. It was expected [28]-[30] that a similar quenching pattern should also be observed for heavy quark (c or b) jet fragmentation. However, in [31] it was pointed out that the a large quark mass would lead to a “dead cone” effect, reducing induced radiation inside the cone $\theta < M/E$ and that this should reduce radiative energy loss of heavy quarks as compared to light partons. Numerical estimates indicated that the quenching of heavy charm quarks may be only about a half that of light quarks. PHENIX

data, however, suggest that the charm quark energy loss could be even smaller than that. In I [14] we showed that the apparent null effect observed for heavy quark energy loss via single electrons may in part be due to a further reduction of the leading order $O(\chi^0)$ associated. In this sense, there are two opposing medium effects: (1) at $O(\chi^0)$ the Ter-Mikayelian (plasmon) effect that arises at 1-HTL loop level the reduces the associated energy loss and (2) at $O(\chi^{n \geq 1})$ the induced radiative energy loss that increases the total radiative energy loss. Our method of calculating the Ter-Mikayelian effect in QCD is discussed in detail below.

In [31] the absence of radiation below a plasma frequency cutoff was estimated to reduce the induced energy loss by only $\sim 10\%$. However, the Ter-Mikayelian effect on the zeroth order in opacity $(L/\lambda)^0$ associated radiation was not considered up to now. The first estimates of the influence of a plasma frequency cutoff in QCD plasmas were reported in [32, 33] using a constant plasmon mass ω_0 [34]-[36]. The k dependence of the gluon self energies and the magnitude of longitudinal radiation were not investigated in that work. We extend those results by taking both longitudinal as well as transverse modes consistently into account via the frequency and wavenumber dependent hard thermal (1-loop HTL) self energy $\Pi^{\mu\nu}(\omega, \vec{k})$ [37]-[41].

As noted in I [14], the dielectric properties of an isotropic plasma lead to a transverse gluon self energy $\Pi_T(\omega, \vec{k})$ with $\Pi_T(\omega_{pl}(0), 0) = \omega_{pl}^2(0) \approx \mu^2/3$, where $\mu \approx gT$ is the Debye screening mass of a plasma at temperature T in the deconfined phase. In addition, long wavelength collective longitudinal gluon modes arise with $\Pi_L(\omega_{pl}(0), 0) = \omega_{pl}^2(0)$. This dynamical gluon mass, $\sqrt{(\omega_{pl}^2(k) - k^2)}$, suppresses not only the radiation of sub-plasmon $\omega < \omega_{pl}(|\vec{k}|)$ gluons but also shields against the collinear $k_\perp \rightarrow 0$ singularities.

In this paper we study under what conditions the assumption of using a k independent effective plasmon mass and neglecting longitudinal modes may be adequate. We show below that this simplifying assumption is surprisingly accurate ($\sim 10\%$) if the asymptotic mass [40], $\omega_\infty = m_E/\sqrt{2}$ rather than the $k = 0$ $\omega_{pl} = \sqrt{2/3}\omega_\infty$ is employed. The accuracy of the approximation also improves dramatically as the mass of the heavy quark increases.

2 Jet Production in the Vacuum

In order to introduce the method that we use to compute the QCD analog of the Ter-Mikayelian [12]-[13] effect on the zeroth order in opacity radiation, we consider first the well known case of radiation in the vacuum.



FIG. 1 Illustration of a bare jet vacuum to vacuum amplitude.

The vacuum to vacuum amplitude, illustrated in Fig.1, is given by

$$-iM_0 = \frac{d_J}{2} \int \frac{d^4 p}{(2\pi)^4} |J(p)|^2 \Delta_M(p) \quad (1)$$

where $\Delta_M(p) = (p^2 + M^2 + i\epsilon)^{-1}$ is the jet propagator for a spinless parton of mass M in the d_J dimensional representation of $SU(N_c)$. We will ignore spin effects throughout since they are irrelevant in the soft radiation limit. The effective jet source current, J , creates an invariant distribution of jets as given by

$$2\text{Im}M_0 = \int d^3 N_J = \int \frac{d^3 \vec{p}}{E_p} E_p \frac{d^3 N_J}{d^3 \vec{p}}, \quad (2)$$

where $E_p d^3 N_J / d^3 \vec{p} = d_J |J(E_p, \vec{p})|^2 / (2(2\pi)^3)$ with $E_p^2 = M^2 + \vec{p}^2$.

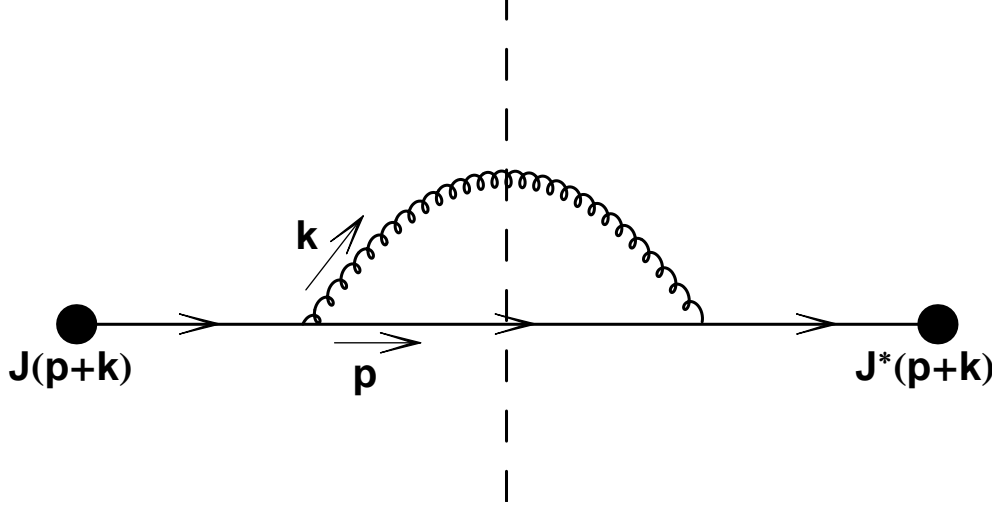


FIG. 2 The one gluon *associated* radiation amplitude in the vacuum.

The one gluon radiative correction amplitude, iM_1 , to the jet spectrum in the vacuum is illustrated on Fig.2

$$-iM_1 = -\frac{g_s^2 C_J d_J}{2} \int \frac{d^4 p}{(2\pi)^4} \frac{d^4 k}{(2\pi)^4} |J(p+k)|^2 \Delta_M(p+k)^2 \Delta_M(p) (2p+k)^\mu D_{\mu\nu}^{(0)}(k) (2p+k)^\nu. \quad (3)$$

The free gluon propagator in the axial ($u_\mu A^\mu = 0$) gauge is

$$D_{\mu\nu}^{(0)}(k) = -\left(g^{\mu\nu} - \frac{u^\mu k^\nu + k^\mu u^\nu}{(uk)} + u^2 \frac{k^\mu k^\nu}{(uk)^2} \right) \Delta_m(k), \quad (4)$$

where m is an infrared mass in the massive gluon scheme introduced by need to study the $m = 0$ limit. In the next section, the dynamic polarization tensor will replace m .

The imaginary part of this amplitude contains real and virtual radiation corrections to iM_0 . The inelastic one gluon radiation contribution is obtained by the Cutkosky rule [45]

$$\Delta_M(p) \Delta_m(k) \rightarrow (-2\pi i)^2 \delta(k^2 - m^2) \delta(p^2 - M^2). \quad (5)$$

This gives a contribution the jet plus gluon production rate

$$\begin{aligned} 2\text{Im}M_1|_{rad} &= \int \frac{d^4 p}{(2\pi)^3} \delta(p^2 - M^2) d_J \int \frac{d^4 k}{(2\pi)^3} \delta(k^2 - m^2) |J(p+k)|^2 \\ &\times \frac{C_J g_s^2}{(Q^2 - M^2)^2} \left\{ (Q^2 - M^2) \frac{4(pu)}{(uk)} - (Q^2 - M^2)^2 \frac{u^2}{(uk)^2} - 4M^2 + m^2 \right\}, \end{aligned} \quad (6)$$

where

$$Q^2 = (p+k)^2 = 2(pk) + k^2 + M^2. \quad (7)$$

In general, the result depends on the gauge parameter u^μ because the external color source J breaks gauge invariance. However, in the soft gluon limit, $k_\perp \ll k^+ \ll p^+$, where k_\perp is measured relative to the \vec{p} axis of the jet, one can extract the familiar DGLAP soft radiation spectrum with any u^μ for which $(uk)/(up) \approx k^+/p^+ = x \ll 1$. For typical light cone kinematics of interest, the momenta

are expressed as

$$\begin{aligned}
k^\mu &= [xE^+, (k_\perp^2 + m^2)/xE^+, \mathbf{k}_\perp] \\
p^\mu &= [(1-x)E^+, (M^2 + k_\perp^2)/(1-x)E^+, -\mathbf{k}_\perp] \\
2pk &= \frac{k_\perp^2 + (1-x)^2m^2 + x^2M^2}{x(1-x)} \\
Q^2 &= pk + m^2 + M^2 = \frac{k_\perp^2 + (1-x)m^2 + xM^2}{x(1-x)} .
\end{aligned} \tag{8}$$

Note that the vertex factor $\{\dots\}$ in Eq. (6) reduces to $(2pk + m^2)/x$ in the $x \rightarrow 0$ limit in both the $A^+ = 0$ light cone and temporal $A^0 = 0$ gauges.

We assume that J is slowly varying $J(p+k) \approx J(p)$ for soft radiation, and therefore, in soft radiation approximation the spectrum can be extracted as

$$2\text{Im}M_1|_{rad} \approx \int d^3N_J \int d^3N_g^{(0)} , \tag{9}$$

leading to the finite mass generalization of the small x invariant DGLAP radiation spectrum

$$\omega \frac{dN_g^{(0)}}{d^3\mathbf{k}} \approx x \frac{dN_g^{(0)}}{dx d^2\mathbf{k}_\perp} \approx \frac{C_J \alpha_s}{x\pi^2(Q^2 - M^2)} = \frac{C_J \alpha_s}{\pi^2} \frac{1}{k_\perp^2 + (1-x)m^2 + x^2M^2} . \tag{10}$$

3 Ter-Mikayelian effect

In this section we want to compute (zeroth order in opacity) associated radiative quark energy loss. In soft gluon limit, the result should not depend on the choice of gauge, as long as $(uk)/(up) \approx x \ll 1$ is satisfied. We simplify our calculations by choosing the temporal axial gauge. However, we have explicitly checked that, in soft gluon limit, the same result is obtained using the light cone gauge.

The radiative heavy quark energy loss in hot dense medium involves both transverse and longitudinal gluon radiation. In temporal axial gauge gluon propagator has the following form (see appendix A):

$$D_{\mu\nu} = -\frac{P_{\mu\nu}}{\omega^2\epsilon_T - \mathbf{k}^2} - \frac{Q_{\mu\nu}}{\omega^2\epsilon_L}, \tag{11}$$

where transverse ($P_{\mu\nu}$) and longitudinal ($Q_{\mu\nu}$) projectors are given in terms of $\bar{g}_{\mu\nu} = g_{\mu\nu} - \frac{k_\mu k_\nu}{k^2}$ and $\bar{u}_\mu = \bar{g}_{\mu\nu} u_\nu$, by

$$P_{\mu\nu} = \bar{g}_{\mu\nu} - \frac{\bar{u}_\mu \bar{u}_\nu}{\bar{u}^2}, \tag{12}$$

$$Q_{\mu\nu} = (g_{\mu\nu} - \frac{u_\mu k_\nu + k_\mu u_\nu}{(u \cdot k)} + \frac{u^2 k_\mu k_\nu}{(u \cdot k)^2} - P_{\mu\nu}) \frac{(u \cdot k)^2}{k^2 u^2} \tag{13}$$

and

$$\epsilon_T = 1 - \frac{\mu^2}{2\mathbf{k}^2} \left(1 - \frac{\omega^2 - \mathbf{k}^2}{2\omega|\mathbf{k}|} \log\left(\frac{\omega + |\mathbf{k}|}{\omega - |\mathbf{k}|}\right)\right), \tag{14}$$

$$\epsilon_L = 1 + \frac{\mu^2}{\mathbf{k}^2} \left(1 - \frac{\omega}{2|\mathbf{k}|} \log\left(\frac{\omega + |\mathbf{k}|}{\omega - |\mathbf{k}|}\right)\right) \tag{15}$$

are transverse and longitudinal dielectric functions respectively [41].

In order to compute the associated radiative energy loss when the hard process is embedded in a dielectric medium, we need to compute the squared amplitude of Feynman diagram $|M_{rad}|$, which represents the source J that produces an off-shell jet with momentum p' , which subsequently radiates a gluon obeying the dispersion relation, $\omega(k)$, of the medium with momentum k . The jet emerges with momentum p and mass M . Since our focus is on heavy quarks, we neglect the thermal shifts of the heavy quark mass here. To calculate this rate we use the optical theorem via

$$\int |M_{rad}|^2 \frac{d^3 \vec{p}}{(2\pi)^3 2E} \frac{d^3 \vec{k}}{(2\pi)^4 2\omega} = 2\text{Im}M_{TM} = \int d^3 N_J \int d^3 N_g^{TM}, \quad (16)$$

where, in axial gauge, $\text{Im}M_{TM}$, is the imaginary part one Hard Thermal Loop amplitude of the diagram cut as shown in Fig.3.

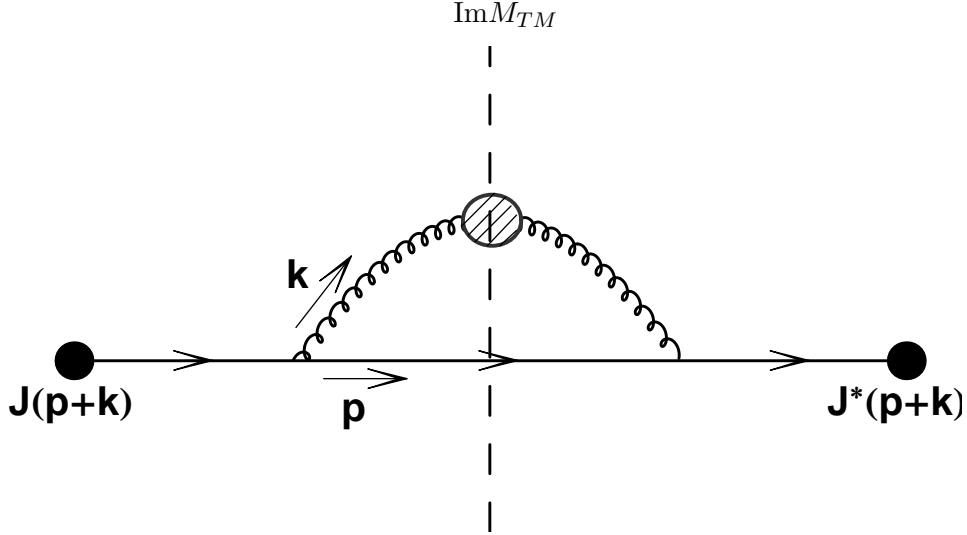


FIG. 3 shows the cut amplitude that contributes to the associated radiative energy loss in the medium. The dashed line shows which propagators are to be put on-shell with respect to the dispersion in the medium. The blob denotes the resummed HTL self energy using Eq. (11, 14, 15).

We assume, as in [4], that J varies slowly with p , i.e. that $J(p+k) \approx J(p)$ and neglect high x spin effects. amplitude in Fig.3 before cutting is

$$-iM = -\frac{C_R D_R}{2} \int \frac{d^4 p}{(2\pi)^4} \frac{d^4 k}{(2\pi)^4} |J(p)|^2 g_s^2 \frac{1}{(Q^2 - M^2)^2} \frac{1}{p^2 - M^2 + i\epsilon} (2p+k)^\mu D_{\mu\nu} (2p+k)^\nu. \quad (17)$$

The contribution to medium on-shell radiation is

$$2\text{Im}M_{TM} = iC_R D_R \int \frac{d^3 p}{(2\pi)^3 2E} |J(p)|^2 \frac{d^4 k}{(2\pi)^4} g_s^2 \frac{1}{(Q^2 - M^2)^2} (2p+k)^\mu D_{\mu\nu} (2p+k)^\nu \quad (18)$$

where we have used [45] $1/(p^2 - M^2 + i\epsilon) \rightarrow (-2\pi i)\delta(p^2 - M^2)$ for the cut quark propagator in Fig.3 (neglecting its small thermal shift). As shown in Appendix B,, the contour integration over ω for on-shell quark and glue is equivalent to replacing $D_{\mu\nu}$ by:

$$D_{\mu\nu} \rightarrow -P_{\mu\nu}(-2\pi i)\delta(\omega^2 \epsilon_T - \vec{k}^2) - \frac{Q_{\mu\nu}}{\omega^2}(-2\pi i)\delta(\epsilon_L), \quad (19)$$

where we only keep positive energy contribution. A small $O(m_g/E)$ quasi elastic contribution is neglected in this approximation as discussed in App. B. We obtain in this way

$$\begin{aligned} \int d^3 N_J \int d^3 N_g^{TM} &= \int \frac{d^3 \vec{\mathbf{p}}}{(2\pi)^3 2E} D_R |J(p)|^2 \int C_R g_s^2 \frac{d^4 k}{(2\pi)^3} \frac{1}{(Q^2 - M^2)^2} \times \\ &\times (2p + k)^\mu (-P_{\mu\nu} \delta(\omega^2 \epsilon_T - \vec{\mathbf{k}}^2) - \frac{Q_{\mu\nu}}{\omega^2} \delta(\epsilon_L)) (2p + k)^\nu \end{aligned} \quad (20)$$

It is convenient to choose coordinates such that $p = (E, |\vec{\mathbf{p}}|, 0, 0)$, where $E = \sqrt{\vec{\mathbf{p}}^2 + M^2}$, and $k = (\omega, |\vec{\mathbf{k}}| \cos \theta, |\vec{\mathbf{k}}| \sin \theta, 0)$. With this kinematics we get:

$$\begin{aligned} (2p + k)^\nu P_{\nu\rho} (2p + k)^\rho &= -(2p + k)^i (\delta_{ij} - \frac{k_i k_j}{\vec{\mathbf{k}}^2}) (2p + k)^j = -4\vec{\mathbf{p}}^2 \sin^2 \theta \\ (2p + k)^\nu Q_{\nu\rho} (2p + k)^\rho &= -(2p + k)^i (\frac{k_i k_j}{\vec{\mathbf{k}}^2}) (2p + k)^j = -(2|\vec{\mathbf{p}}| \cos \theta + |\vec{\mathbf{k}}|)^2. \end{aligned} \quad (21)$$

The integrated radiation yield than becomes:

$$\begin{aligned} \int d^3 N_g^{TM} &= \int d\omega d\cos\theta d\vec{\mathbf{k}}^2 d|\vec{\mathbf{k}}| \frac{C_R \alpha_S}{\pi} \frac{1}{(Q^2 - M^2)^2} \times \\ &\times \{4\vec{\mathbf{p}}^2 \sin^2 \theta \delta(\omega^2 \epsilon_T - \vec{\mathbf{k}}^2) + \frac{(2|\vec{\mathbf{p}}| \cos \theta + |\vec{\mathbf{k}}|)^2}{\omega^2} \delta(\epsilon_L)\} \end{aligned} \quad (22)$$

where $Q^2 - M^2 = \omega^2 - \vec{\mathbf{k}}^2 + 2(E\omega - |\vec{\mathbf{p}}||\vec{\mathbf{k}}| \cos \theta)$, as in Eq. (7).

The Ter-Mikayelian modified associated (0^{th} order in opacity) radiative energy loss spectrum is defined as $dI_g = \omega d^3 N_g^{TM}$. Using this, the transverse and longitudinal contribution to the 0^{th} order radiated energy loss per wave number is given by the following:

$$\begin{aligned} \frac{dI_T}{d|\vec{\mathbf{k}}|} &= \frac{C_F}{\pi} \frac{4\vec{\mathbf{k}}^2 \vec{\mathbf{p}}^2 \omega_T^2 (\omega_T^2 - \vec{\mathbf{k}}^2)}{\omega_T^2 \mu^2 - (\omega_T^2 - \vec{\mathbf{k}}^2)^2} \int_0^1 d\cos\theta \frac{\alpha_S (Q^2 - M^2)}{(Q^2 - M^2)^2} \sin^2 \theta \\ \frac{dI_L}{d|\vec{\mathbf{k}}|} &= \frac{C_F}{\pi} \frac{4\vec{\mathbf{k}}^2 \vec{\mathbf{p}}^2 (\omega_L^2 - \vec{\mathbf{k}}^2)}{\mu^2 - (\omega_L^2 - \vec{\mathbf{k}}^2)} \int_0^1 d\cos\theta \frac{\alpha_S (Q^2 - M^2)}{(Q^2 - M^2)^2} \left(\cos\theta + \frac{\vec{\mathbf{k}}^2}{2\vec{\mathbf{p}}^2} \right)^2 \end{aligned} \quad (23)$$

where we keep only the forward, $\theta > 0$, emission to isolate the energy loss of the nearside jet. In Eq. (23) ω_T and ω_L are positive zeros of $(\omega^2 \epsilon_T - \vec{\mathbf{k}}^2)$ and ϵ_L respectively. The angular integration can be performed analytically if α_S does not run, but it is not particularly useful. We perform the integration using no momentum cutoffs and running coupling according to the "Frozen α model" [46]

$$\alpha_S(Q^2 - M^2) = \text{Min}\left\{0.5, \frac{4\pi}{\beta_0 \text{Log}\left(\frac{Q^2 - M^2}{\Lambda_{QCD}^2}\right)}\right\}, \quad (24)$$

where $\beta_0 = \frac{28}{3}$ for effective number of flavors $n_f \approx 2.5$ and $\Lambda_{QCD} \approx 0.2$ GeV. Figures 4 and 5 show transverse and longitudinal contribution to the charm and bottom radiative energy loss at different Debye masses.

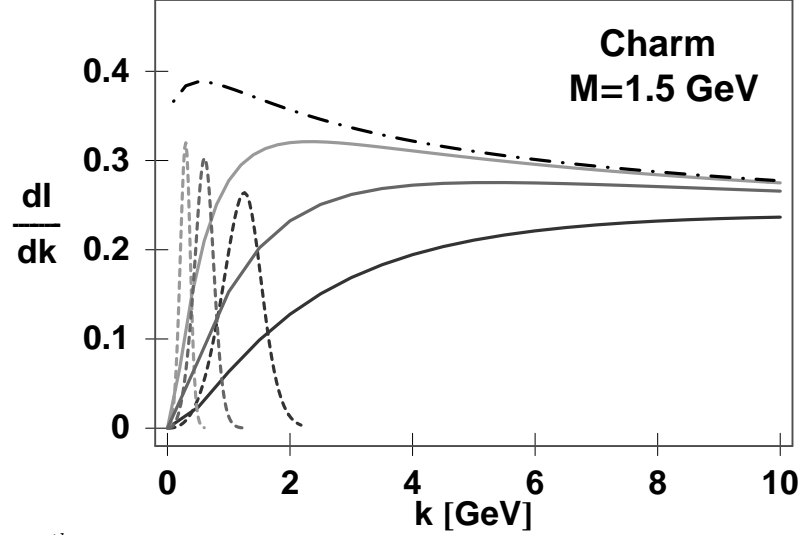


FIG. 4 The 0^{th} order in opacity contribution to Charm quark radiated energy loss for 15 GeV jet is shown as a function of wave number. The dashed-dotted curve shows what would the energy loss be if gluons were treated as massless and transversely polarized. From top to bottom (left to right) solid (dashed) curves show medium modified transverse (longitudinal) contribution to the energy loss for Debye mass 0.25 GeV, 0.5 GeV and 1 GeV respectively.

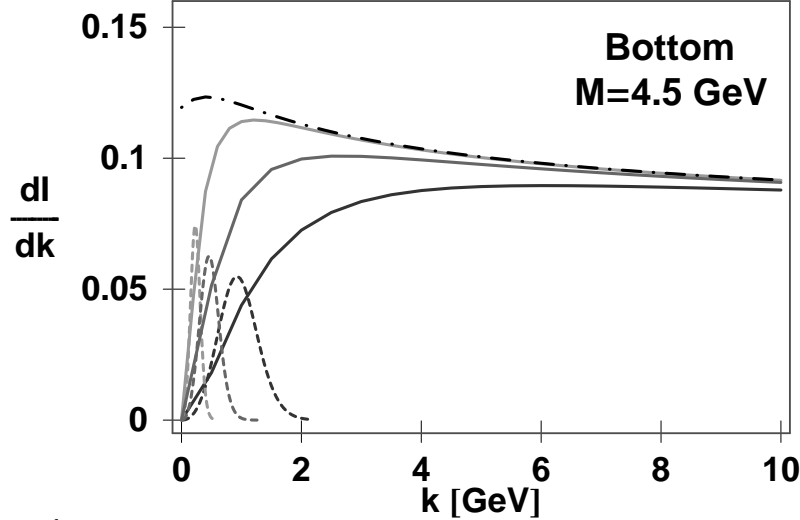


FIG. 5 The 0^{th} order in opacity contribution to Bottom quark radiated energy loss for 15 GeV jet is shown as a function of wave number. The dashed-dotted curve shows what would the energy loss be if gluons were treated as massless and transversely polarized. From top to bottom (left to right) solid (dashed) curves show medium modified transverse (longitudinal) contribution to the energy loss for Debye mass 0.25 GeV, 0.5 GeV and 1 GeV respectively.

We see that longitudinal contribution to the energy loss is significant only in the ω region around Debye mass. As temperature T of the medium increases the transverse contribution to the energy loss decreases, while longitudinal contribution increases. Therefore, we can conclude that for lower Debye masses (lower temperatures) the longitudinal contribution to the energy loss is negligible, but at high enough temperatures it may become comparable to the transverse contribution.

Fig.6 shows the integrated 0^{th} order fractional energy loss for charm and bottom quarks in a hot plasma with Debye mass $\mu = 0.5$ GeV.

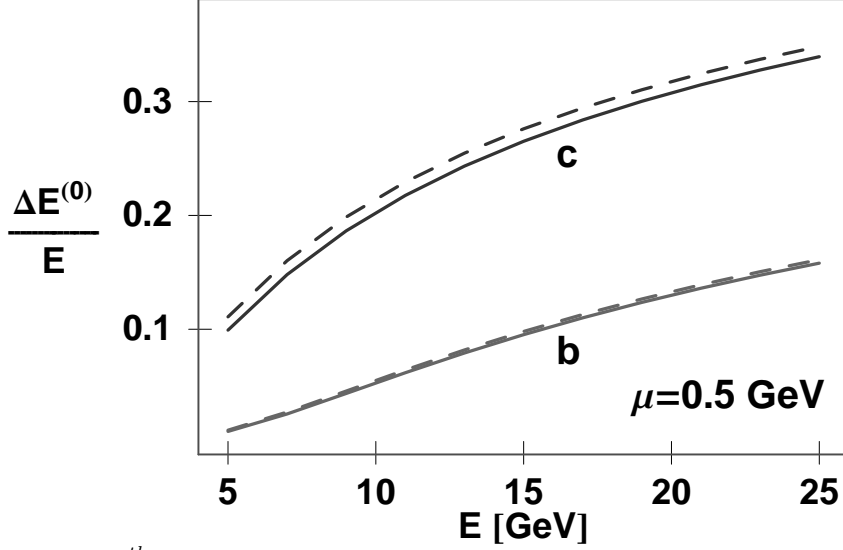


FIG. 6 The 0^{th} order in opacity fractional energy loss for charm and bottom quarks in hot medium with Debye mass $\mu = 0.5$ GeV, and zero momentum cutoff is shown as a function of the charm quark energy. The upper (lower) solid curve shows transverse fractional energy loss for charm (bottom) quark. The dashed curves show the negligible additional effect of longitudinal plasmons.

We see that the longitudinal plasmon contribution is indeed negligible for both charm and bottom quarks.

In order to study in more detail how the specific 1-loop HTL dispersion relation affects the results we show in Fig. 7 the dynamical gluon mass as a function of wavenumber for different screening scales.

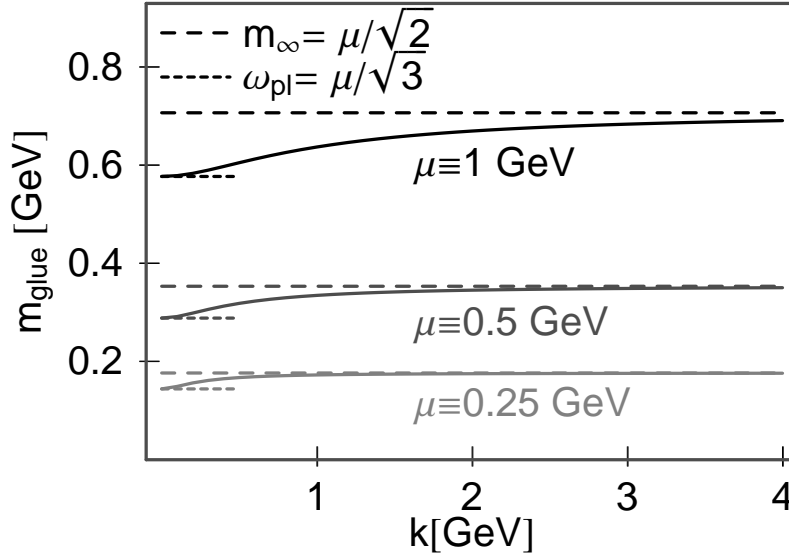


FIG. 7 One loop transverse plasmon mass $m_g(|\vec{k}|) \equiv \sqrt{\omega^2 - \vec{k}^2}$ is shown as a function of quark momentum $|\vec{k}|^2$. We see that m_g starts with the value $\omega_{pl} = \mu/\sqrt{3}$ at low $|\vec{k}|$, and that as $|\vec{k}|$ grows, m_g asymptotically approaches the value of $\omega_\infty = \mu/\sqrt{2}$ in agreement with [40].

The main feature to note is the relatively rapid transition from the static $\omega_{pl} = \mu/\sqrt{3}$ to an asymptotic

$m_\infty = \mu/\sqrt{2}$ as emphasized in [40]. The effect of replacing the dynamical mass by a single effective value, either ω_{pl} , m_∞ , or μ is shown in Fig.8.

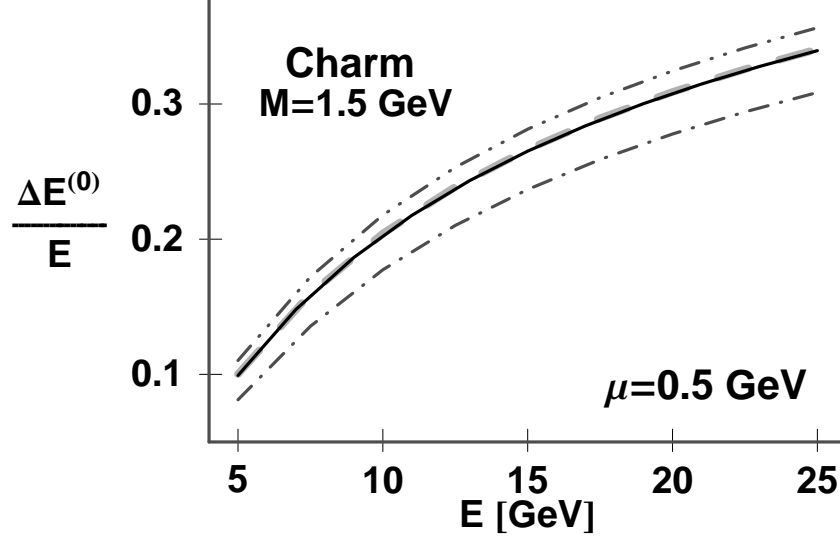


FIG. 8 Medium modified zeroth order in opacity charm quark fractional energy loss is shown as a function of quark energy. Full curve shows the transverse energy loss using Eq. (23). Dot-dot-dashed, dashed and dot-dashed curves show what would be the transverse energy loss if we define gluon mass as ω_{pl} , m_{infty} and μ respectively.

Figs. 7,8 demonstrate that a remarkably good approximation to the the Ter-Mikayelian effect can be obtained by approximating $m_q(k) \approx m_\infty$ (see also Appendix B1).

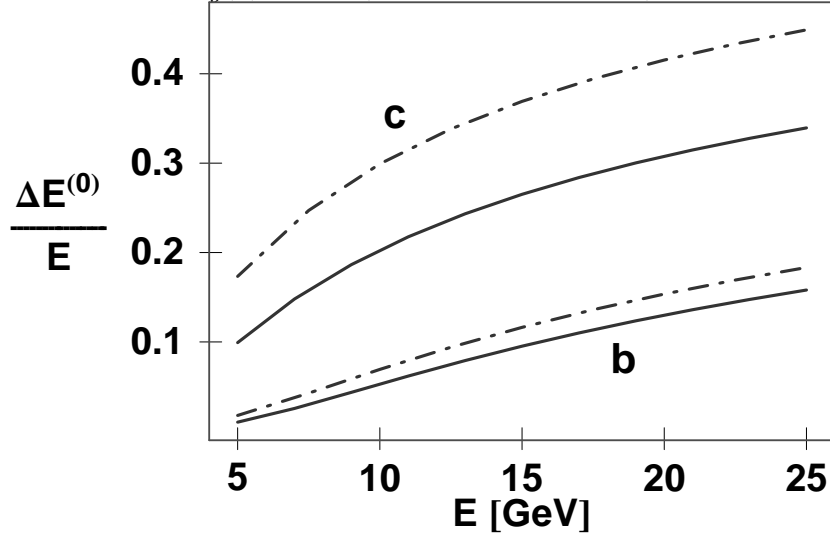


FIG. 9 The reduction of the fractional associated vacuum energy loss for charm and bottom quark due to the QCD Ter-Mikayelian plasmon effect is shown as a function of the quark energy. The upper (lower) dashed-dotted curve shows the vacuum energy loss for charm (bottom) quark if gluons are treated as massless and transversely polarized. The upper (lower) solid curve shows the effect of using the medium dispersion for gluons. We take $\mu = 0$ GeV for the vacuum and $\mu = 0.5$ GeV for the medium cases.

In Fig. 9 we compare the associated energy loss in the vacuum and a medium with $\mu = 0.5$ GeV. We see that for charm quark medium energy loss is significantly reduced by $\approx 30\%$. The Ter-Mikayelian

plasmon effect therefore *enhances* the yield of high transverse charm quarks relative to the vacuum case. On the other hand, we see that for bottom quark Ter-Mikayelian effect is negligible as is the absolute associated radiated energy because the dead cone [31] is so wide in that case.

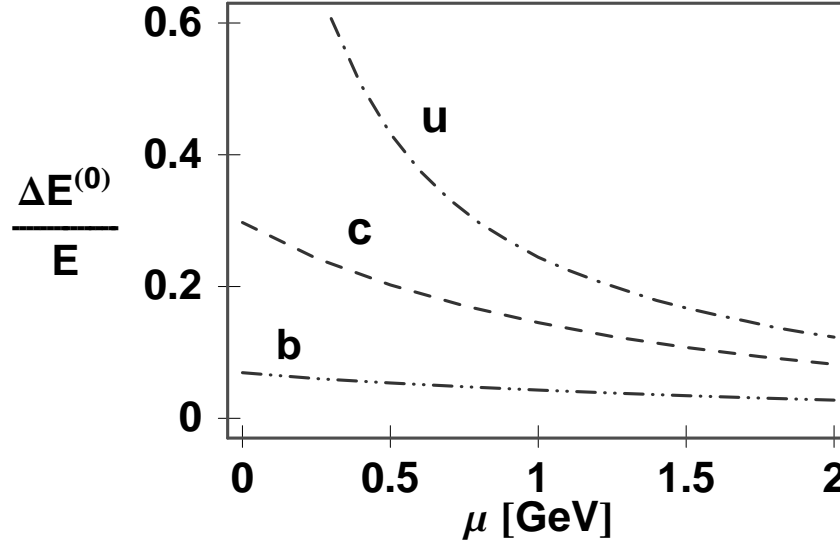


FIG. 10 Medium modified zeroth order in opacity fractional energy loss is shown as a function of Debye mass μ for different mass quarks. We see that medium effect is more important for light (dot-dashed curve) and charm (dashed curve) quark energy loss, since it leads to the strong suppression of the associated radiation. On the other hand, bottom quark (dot-dot-dashed curve) energy loss shows only a weak dependence on the medium.

So far, we have concentrated on the Ter-Mikayelian effect for only heavy quarks. The generalization of the plasmon effect to light quarks is not trivial due to the fact that the light quark vacuum energy loss is infrared divergent. However, as shown in Fig.10 we see that in a QCD medium, dynamic polarization naturally regulates infrared divergences for light quarks, since both quarks [47, 48] and gluons acquire a finite self energy. Confinement in the vacuum naturally limits the effective screening scale to $\mu_{vac} > \Lambda_{QCD}$.

4 Conclusion

In this paper we computed both the transverse and longitudinal contributions to the lowest order in opacity radiative quark energy loss. We have shown that longitudinal contribution can be neglected for the energy range of experimental interest. We have also seen that transverse polarization can be, for moderate range of temperatures ($0.5 \leq \mu \leq 1$ GeV), approximated by simple form $D_{\mu\nu} \approx -\frac{P_{\mu\nu}}{k^2 - m_g^2}$, where $P_{\mu\nu}$ is transverse projector and $m_g \approx m_\infty = \mu/\sqrt{2}$. It is remarkable how well the effect of medium polarization $\Pi_{\mu,\nu}(\omega, \vec{k})$ can be approximated numerically in this simple way. In a subsequent paper [44], we will use this approximation to simplify the calculations of medium induced radiative energy loss.

In the appendix B it was also seen that the poles of the gluon propagator give both the contribution from quasi-particles and "particle hole excitations" (which correspond to the energy ω smaller than momentum $|\vec{k}|$). However, we have shown that the particle hole contribution to the radiative energy loss is negligible compared to the radiative one.

The next step beyond the 1 loop HTL approximation employed here will be to compute the 2 loop (1st order in opacity corrections) to the associated energy loss. Cutting two HTL loops diagrams, we

pick up three different contributions to the energy loss. Two of them give corrections to the plasmon mass and particle hole energy loss respectively. These are perturbative higher order corrections to the results here. However, a third contribution, in which the poles of two HTL propagators give one quasi-particle and one particle-hole excitation give rise to additional energy loss. This contribution corresponds to the generalization of the first order opacity correction to medium induced radiative energy loss computed for light partons in [4]. The results were summarized in I [14], and the details of that computation will be reported in a subsequent paper [44].

Acknowledgments: Valuable discussions with I. Vitev, Z. Lin, J. Nagle, and W. Zajc on heavy quark production at RHIC are gratefully acknowledged. This work is supported by the Director, Office of Science, Office of High Energy and Nuclear Physics, Division of Nuclear Physics, of the U.S. Department of Energy under Grant No. DE-FG02-93ER40764.

A Gluon propagator in temporal axial gauge

We recall here some of the basic tensorial properties of the gluon propagator, in axial gauges ($u^\mu A_\mu(\vec{x}, t) = 0$, u^μ a fixed four vector).

The transverse projector $P^{\mu\nu}$ (with respect to both k^μ and u^μ), is given by Eq. (12). Note that $\bar{u}^2 = u^2 - (ku)^2/k^2$ is well defined even in light cone ($u^2 = 0$) gauge.

The orthogonal longitudinal projector, $Q^{\mu\nu}$ (with respect to k^μ), is given by

$$\begin{aligned} Q_{\mu\nu} &= \left(g_{\mu\nu} - \frac{u_\mu k_\nu + k_\mu u_\nu}{(u \cdot k)} + \frac{u^2 k_\mu k_\nu}{(u \cdot k)^2} - P^{\mu\nu} \right) \frac{(u \cdot k)^2}{k^2 u^2} \\ &= \left(\frac{u^\mu u^\nu}{u^2} (uk)^2 + k^\mu k^\nu u^2 - (u^\mu k^\nu + k^\mu u^\nu)(uk) \right) \frac{1}{u^2 k^2 - (uk)^2} \end{aligned} \quad (25)$$

In terms of these projectors the free gluon propagator in the axial gauge is

$$\begin{aligned} D^{(0)\mu\nu}(k) &= -\Delta(k) (P^{\mu\nu} + \beta(k, u) Q^{\mu\nu}) \\ &= -\frac{1}{k^2 + i\epsilon} \left(g^{\mu\nu} - \frac{u^\mu k^\nu + k^\mu u^\nu}{(uk)} + u^2 \frac{k^\mu k^\nu}{(uk)^2} \right) \end{aligned} \quad (26)$$

where

$$\beta(k, u) = \frac{k^2 u^2}{(uk)^2} . \quad (27)$$

is a kinematic factor. In the temporal axial gauge, $u = (1, 0, 0, 0)$, $\beta = 1 - \mathbf{k}^2/\omega^2$ and the projectors reduce to

$$\begin{aligned} P_{\mu\nu} &= Q_{\mu\nu} = 0, \text{ if } \mu, \nu = 0 \\ P_{ij} &= -\delta_{ij} + \frac{k_i k_j}{\vec{k}^2}, \quad Q_{ij} = -\frac{k_i k_j}{\vec{k}^2}, \text{ if } i, j = 1, 2, 3. \end{aligned} \quad (28)$$

In a medium with four velocity u^μ the gluon acquires a temperature dependent self energy $\Pi_{\mu\nu}$ in addition to its vacuum self energy. The one-loop (Hard Thermal Loop [40] (HTL) or equivalently, eikonal linear response [41]) self energy can be decomposed as

$$\Pi_{\mu\nu} = \Pi_L R_{\mu\nu} + \Pi_T P_{\mu\nu} \quad (29)$$

where

$$R_{\mu\nu} = \frac{\bar{u}_\mu \bar{u}_\nu}{\bar{u}^2} \quad (30)$$

is the longitudinal projector in covariant gauges with respect to u^μ but transverse with respect to k^μ . Therefore, the HTL self energy is transverse with respect to k , $k\Pi = \Pi k = 0$. Note that $RP = PR = 0$, $R^2 = R$, and

$$QRQ = Q/\beta(k, u) \quad (31)$$

where β is given by (27).

The HTL medium modified gluon propagator ($D_{\mu\nu}$) can be obtained by solving the Dyson equation [47]

$$\begin{aligned} D_{\mu\nu} &= D_L Q_{\mu\nu} + D_T P_{\mu\nu} = D_{\mu\nu}^{(0)} - D_{\mu\alpha}^{(0)} \Pi^{\alpha\beta} D_{\beta\nu} \\ &= -\frac{P_{\mu\nu}}{\omega^2 \epsilon_T - \vec{k}^2} - \frac{Q_{\mu\nu}}{\omega^2 \epsilon_L} \quad (32) \end{aligned}$$

Note that, in general [41], we would have one extra term $\eta \frac{k_\mu k_\nu}{k^4}$ in the gluon propagator, where η is a gauge parameter. However, in temporal axial gauge [47],

$$D_{\mu\nu} = 0, \text{ if } \mu, \nu = 0.$$

Therefore, in temporal axial gauge η has to be equal to zero, i.e. extra term vanishes.

B Cutkosky rules for gluon propagator in the medium

In this appendix we want to justify using the Cutkosky rules for gluon propagator in the medium, which is represented by Eq. (19) in our computations.

Diagram M

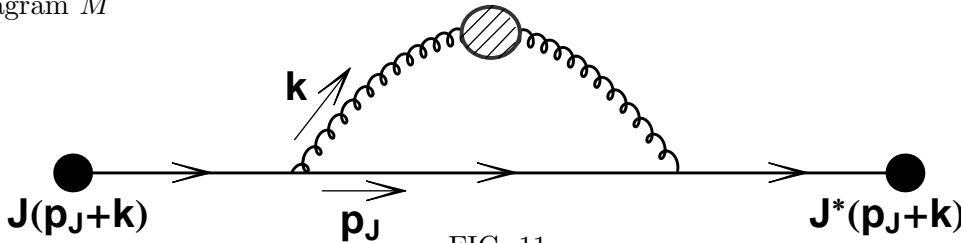


FIG. 11

corresponds to $\sum M_n$, where M_n is the amplitude of the following diagram:

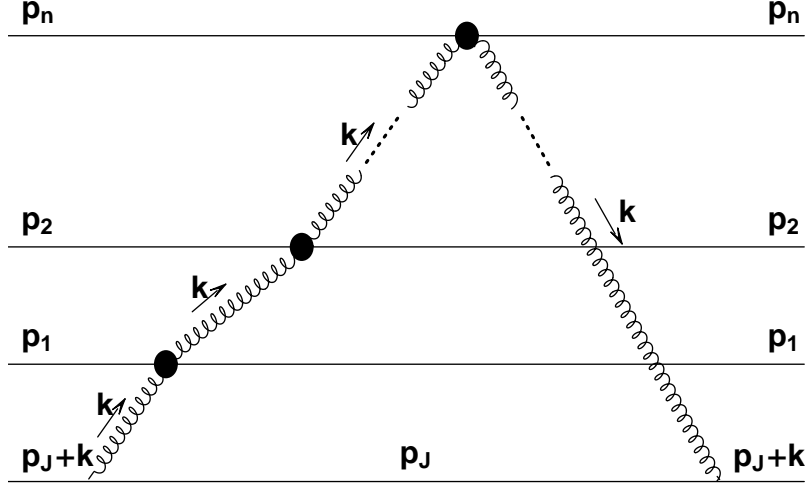


FIG. 12

Here,

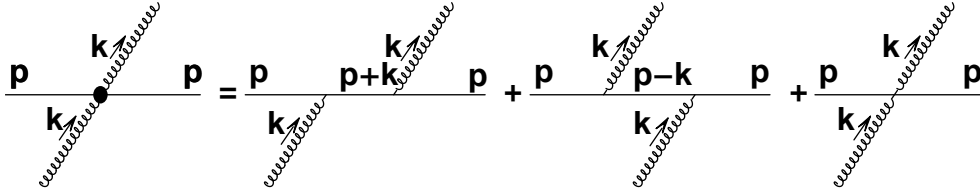


FIG. 13

$$\begin{aligned}
\langle iM_n \rangle &= Tr \left\{ \sum_{a_0} \int \frac{d^4 p_J}{(2\pi)^4} \frac{d^4 k}{(2\pi)^4} |J(p+k)|^2 \frac{1}{((p_J+k)^2 - M^2 + i\epsilon)^2} \frac{i}{p_J^2 - M^2 + i\epsilon} \right. \\
&\quad \times (-ig_s(2p_J+k)^{\mu_0} T_{a_0}) \frac{-ig_{\mu_0\nu_1}}{k^2 + i\epsilon} i\pi^{\nu_1\mu_1} \frac{-ig_{\mu_1\nu_2}}{k^2 + i\epsilon} i\pi^{\nu_2\mu_2} \dots i\pi^{\nu_n\mu_n} \frac{-ig_{\mu_n\nu_0}}{k^2 + i\epsilon} (-ig_s(2p_J+k)^{\nu_0} T_{a_0}) \left. \right\} (33)
\end{aligned}$$

where $\pi^{\mu\nu}(k)$ is the amplitude of the diagram shown on Fig.13, averaged over thermal momentum distribution $n_{eq}(p)$ given by Eq. (35).

$$\begin{aligned}
i\pi^{\mu\nu}(k) &= \int d^4 p n_{eq}(p) \left\{ \frac{i}{(p+k)^2 + i\epsilon} (-ig_s(2p+k)^\mu) (-ig_s(2p+k)^\nu) + \right. \\
&\quad \left. + \frac{i}{(p-k)^2 + i\epsilon} (-ig_s(2p-k)^\mu) (-ig_s(2p-k)^\nu) + 2ig^{\mu\nu} \right\} \sum_j jT_a T_b j^\dagger \quad (34)
\end{aligned}$$

where $\sum_j jT_a T_b j^\dagger = \frac{1}{2}\delta_{ab}$, and $n_{eq}(p)$ is the equilibrium momentum distribution [41] at temperature T including both quarks and gluons

$$n_{eq}(p) = \frac{1}{2}(Q_{eq}^+ + Q_{eq}^-) + NG_{eq}. \quad (35)$$

Here

$$Q_{eq}^\pm = \frac{2N_f}{(2\pi)^3} 2\theta(\pm p^0) \delta(p^2) (\exp(\pm \frac{p^0}{T}) + 1)^{-1} \quad (36)$$

and

$$G_{eq} = \frac{2N}{(2\pi)^3} 2\theta(p^0) \delta(p^2) (\exp(\frac{p^0}{T}) - 1)^{-1} \quad (37)$$

are quark (antiquark) and gluon distributions respectively. N_f is the number of flavors, and N is the number of colors.

In the soft gluon limit $\pi^{\mu\nu}$ becomes

$$\pi^{\mu\nu} = -g_s^2 \int d^4p \frac{p^\mu k_\alpha (p^\alpha \partial_p^\nu - p^\nu \partial_p^\alpha)}{(pk) + i\epsilon} n_{eq}(p), \quad (38)$$

in agreement with [41].

It is easy to prove that $\pi^{\mu\nu}$ is transverse, i.e. $\pi^{\mu\nu} k_\nu = k_\mu \pi^{\mu\nu} = 0$.

Therefore, in covariant gauge $\pi^{\mu\nu}$ can be decomposed:

$$\pi^{\mu\nu} = \Pi_T P^{\mu\nu} + \Pi_L R^{\mu\nu}, \quad (39)$$

where $P^{\mu\nu}$ and $R^{\mu\nu}$ are given by Eqs. (12) and (30) respectively.

Using Eqs. (38, 39, 12, 30) we get

$$\Pi_L = Q_{\mu\nu} \pi^{\mu\nu} = -g_s^2 \frac{k^2}{u^2 k^2 - (ku)^2} \int d^4p (pu) \frac{(pk)(u\partial n) - (pu)(k\partial n)}{(pk)} \quad (40)$$

$$\Pi_T = \frac{1}{2} P_{\mu\nu} \pi^{\mu\nu} = -\frac{1}{2} g_s^2 \int d^4p \frac{1}{(pk)} \left\{ (k\partial n) \left(\frac{k^2 (pu)^2}{u^2 k^2 - (ku)^2} - p^2 \right) + (pk) \left((p\partial n) - \frac{k^2 (pu)(u\partial n)}{u^2 k^2 - (ku)^2} \right) \right\} \quad (41)$$

By replacing $n_{eq}(p)$ from Eq. (35) we get

$$\Pi_L = -\frac{(\omega^2 - \vec{k}^2)\mu^2}{\vec{k}^2} \left(1 + \frac{\omega}{2|\vec{k}|} \log \left| \frac{\omega - |\vec{k}|}{\omega + |\vec{k}|} \right| \right) \quad (42)$$

and

$$\Pi_T = \frac{\mu^2}{2} + \frac{(\omega^2 - \vec{k}^2)\mu^2}{2\vec{k}^2} \left(1 + \frac{\omega}{2|\vec{k}|} \log \left| \frac{\omega - |\vec{k}|}{\omega + |\vec{k}|} \right| \right) \quad (43)$$

where $\mu = g_s T \sqrt{1 + \frac{N_f}{6}}$.

These results are in agreement with [41], and they lead to ϵ_L and ϵ_T which we use in this paper.

Using $\pi^{\mu\nu}$ from Eq. (39) M finally becomes:

$$M = (-i) \int D_R |J(p_J)|^2 \frac{d^4 p_J}{(2\pi)^4} \frac{1}{p_J^2 - M^2 + i\epsilon} \times \\ \times \int C_R g_s^2 \frac{d^4 k}{(2\pi)^4} \frac{1}{((p_J + k)^2 - M^2 + i\epsilon)^2} (2p_J + k)^\mu D_{\mu\nu} (2p_J + k)^\nu \quad (44)$$

where $D_{\mu\nu} = -\frac{P^{\mu\nu}}{k^2 - \Pi_T + i\epsilon} - \frac{Q^{\mu\nu}}{k^2 - \Pi_L + i\epsilon}$, and we assume that ϵ is positive.

Lets now compute

$$\int d\omega \frac{1}{((p_J + k)^2 - M^2 + i\epsilon)^2} (2p_J + k)^\mu D_{\mu\nu} (2p_J + k)^\nu = \int d\omega \left(\frac{f_T(p_J, k)}{k^2 - \Pi_T + i\epsilon} - \frac{f_L(p_J, k)}{k^2 - \Pi_L + i\epsilon} \right) \quad (45)$$

Since we are interested only in the radiative energy loss, we assume that initial jet is off-shell, and therefore we have that $f_T(p_J, k)$ and $f_L(p_J, k)$ are analytic functions.

From Eqs. (40, 41) we see that Π_T and Π_L can be written as $\sum_p \frac{\xi_{T(L)}(p, k)}{(pk)}$ where $\xi_{T(L)}(p, k)$ are analytic functions, and where we have assumed that we have discrete set of p 's.

Since discussion for both parts of the integral (45) is the same, we will consider only one part:

$$\int d\omega \frac{f(p_J, k)}{\omega^2 - \vec{k}^2 - \sum_p \frac{\xi(p, k)}{(pk)} + i\epsilon}. \quad (46)$$

Note that $\frac{\xi(p, k)}{(pk)}$ is infinite when $\omega = \frac{\vec{p} \cdot \vec{k}}{E_p}$.

For simplicity, suppose that all $\frac{\vec{p} \cdot \vec{k}}{E_p}$ are different. We can order them in such a way that $\omega_1 < \omega_2 < \dots < \omega_n \leq |\vec{k}|$.

Than, for fixed $|\vec{k}|$ zeros, $\pm(\Omega_i - i\epsilon)$, of $(\omega^2 - \vec{k}^2 - \sum_p \frac{\xi(p, k)}{(pk)} + i\epsilon)$ can be found graphically:

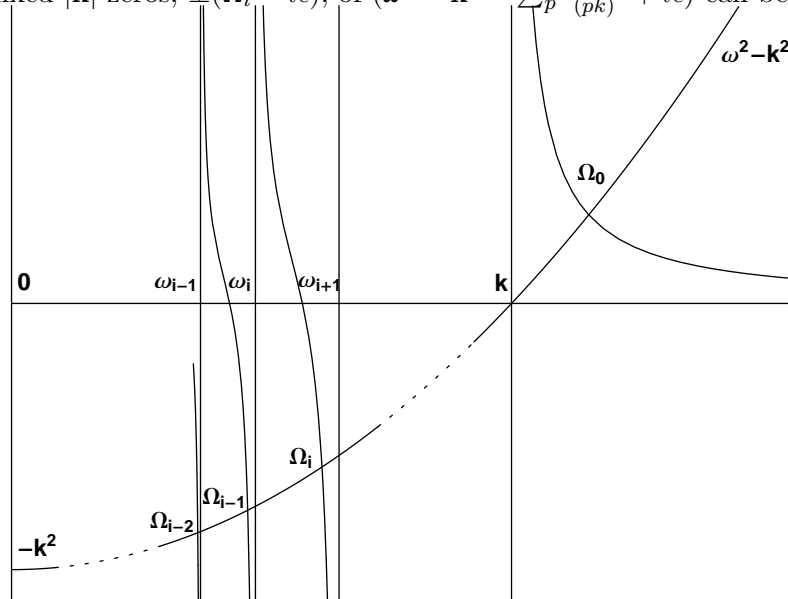


FIG. 14 shows schematically the zeros Ω_i for $\omega^2 - \vec{k}^2 - \sum_p \frac{\xi(p, k)}{(pk)}$ at fixed $|\vec{k}|$.

We see that we have $n' < n$ different solutions $\Omega_i \leq |\vec{\mathbf{k}}|$, and exactly one solution $\Omega_0 > |\vec{\mathbf{k}}|$. Then, if we close the contour in Eq. (46) in clockwise direction, we will pick up only positive poles, i.e. $(\Omega_i - i\epsilon)$.

Therefore,

$$\int d\omega \frac{f(p_J, k)}{\omega^2 - \vec{\mathbf{k}}^2 - \sum_p \frac{\xi(p, k)}{(pk)} + i\epsilon} = (-2\pi i) \sum_{i=1}^{n'} \text{Res}(\Omega_i) + (-2\pi i) \text{Res}(\Omega_0). \quad (47)$$

In the following subsection, we will test the relative magnitude of the two contributions for the case of the dominant transverse excitations. Solutions $\Omega_i < |\vec{\mathbf{k}}|$ correspond to particle hole excitation, and we will prove that this contribution is negligible.

B.1 Simplifying the gluon propagator in hot dense medium

The transverse response

$$\rho_T(k) \equiv \frac{1}{2\pi} \text{Disc} \left[\frac{1}{k^2 - \Pi_T(k)} \right] \quad (48)$$

obeys the sum rule [48]

$$\int_{-\infty}^{\infty} d\omega \omega \rho_T(\omega, |\vec{\mathbf{k}}|) = 1 \quad (49)$$

We can write

$$\rho_T(\omega, |\vec{\mathbf{k}}|) = \beta(\omega, |\vec{\mathbf{k}}|) + \delta(\omega^2 \epsilon_T - \vec{\mathbf{k}}^2), \quad (50)$$

where first part in this formula corresponds to the particle hole excitation, and the second part corresponds to the delta function contribution.

It is easy to show that

$$\delta(\omega^2 \epsilon_T - \vec{\mathbf{k}}^2) = \delta(\omega^2 - \omega_T^2) Z_T(k) \quad (51)$$

where ω_T is the transverse plasmon spectrum, and

$$Z_T(k) = \frac{2\omega_T^2(\omega_T^2 - \vec{\mathbf{k}}^2)}{\omega_T^2 \mu^2 - (\omega_T^2 - \vec{\mathbf{k}}^2)^2}. \quad (52)$$

The sum rule reduces to

$$Z_T(k) + \int_{-\infty}^{\infty} d\omega \omega \beta(\omega, |\vec{\mathbf{k}}|) = 1 \quad (53)$$

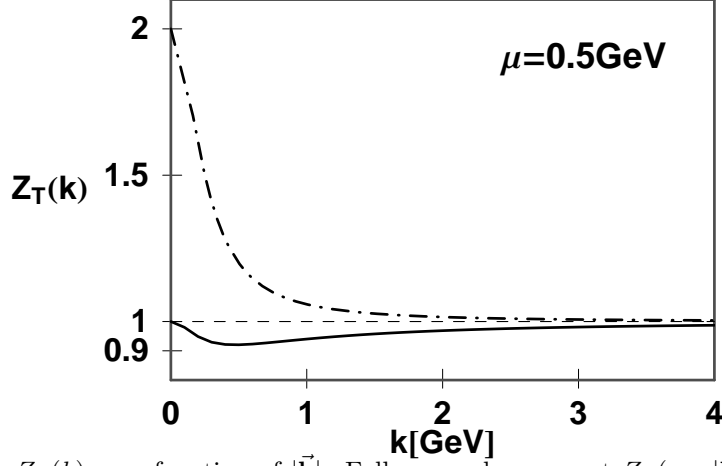


FIG. 15 shows $Z_T(k)$ as a function of $|\vec{k}|$. Full curve shows exact $Z_T(\omega_T, |\vec{k}|)$, while dot-dashed curve shows $Z_T(\sqrt{\vec{k}^2 + m_g^2}, |\vec{k}|)$, in which ω_T is approximated by $\sqrt{\vec{k}^2 + m_g^2}$.

In Fig.15 we see that $Z_T(\omega_T, |\vec{k}|)$ is approximately equal to 1 for whole region of $|\vec{k}|$. Therefore, we can conclude that the contribution from the particle hole excitation is negligible.

In order to justify this conclusion we will estimate the particle hole contribution to the energy loss. For simplicity, we will consider quarks to be massless.

From Eq. (22) we see that

$$\begin{aligned} \frac{\Delta E^{\text{hole}}}{E} &= \int \frac{1}{E} \omega d\omega d\cos\theta \vec{k}^2 d|\vec{k}| \frac{C_{R\alpha S}}{\pi} \frac{1}{(Q^2 - M^2)^2} 4\vec{p}^2 \sin^2\theta \beta(\omega, |\vec{k}|) < \\ &< \frac{2}{E} \frac{C_{R\alpha S}^{\text{max}}}{\pi} \int \vec{k}^2 d|\vec{k}| x dx \beta(x, |\vec{k}|) (\text{Ln}(\frac{1+x}{1-x}) - 2) \end{aligned} \quad (54)$$

where $x \equiv \frac{\omega}{|\vec{k}|}$.

$$(\text{Ln}(\frac{1+x}{1-x}) - 2) < (\text{Ln}(\frac{2}{0.05}) - 2) - \text{Ln}(1-x) \Theta(x - 0.95) \quad (55)$$

Using Eq. (55) we get:

$$\begin{aligned} \frac{\Delta E^{\text{hole}}}{E} &< \frac{2}{E} \frac{C_{R\alpha S}^{\text{max}}}{\pi} \{ (\text{Ln}(\frac{2}{0.05}) - 1) \int d|\vec{k}| \int \vec{k}^2 x dx \beta(x, |\vec{k}|) - \\ &\quad - \int_{0.95}^1 x dx \text{Ln}(1-x) \int_0^{|\vec{p}|} d|\vec{k}| \vec{k}^2 \beta(x, |\vec{k}|) \} < \\ &< \frac{2}{E} \frac{C_{R\alpha S}^{\text{max}}}{\pi} \{ 2 \int_0^{|\vec{p}|} d|\vec{k}| \frac{(1 - Z_T(k))}{2} - \int_{0.95}^1 x dx \text{Ln}(1-x) \int_0^{|\vec{p}|} d|\vec{k}| \vec{k}^2 \beta(x, |\vec{k}|) \} \end{aligned} \quad (56)$$

where in the first integral we have used Eq. (53).

Using the fact that $|1 - Z_T(k)| \sim \frac{m_g^2}{2(\vec{k}^2 + m_g^2)}$ we get

$$\frac{2}{E} \frac{C_R \alpha_S^{\max}}{\pi} \int_0^{|\vec{p}|} d|\vec{k}| (1 - Z_T(k)) \approx \frac{C_R \alpha_S^{\max}}{\pi} \frac{m_g}{E} \frac{\pi}{2} \quad (57)$$

In the $x \rightarrow 1$ region $\beta(x, |\vec{k}|)$ [48] can be approximated by

$$\beta(x, |\vec{k}|) \approx \frac{m_g^2 (1 - x)}{(2\vec{k}^2 (1 - x) + m_g^2)^2} \quad (58)$$

Then, the second integral in Eq. (56) can be performed analytically, leading to:

$$\frac{\Delta E^{\text{hole}}}{E} < C_R \alpha_S^{\max} \frac{m_g}{E} \quad (59)$$

We see that the particle hole contribution to the fractional energy loss is on the order (m_g/E) . Since $m_g \ll E$ we can conclude that this contribution is negligible.

Finally, on Fig.7 we saw that $\omega_T \approx \sqrt{\vec{k}^2 + m_g^2}$. Dot-dashed curve on Fig.15 represents $Z_T(\sqrt{\vec{k}^2 + m_g^2}, |\vec{k}|)$ as a function of $|\vec{k}|$. Again, with the exception of the small $|\vec{k}| < 1$ GeV region, we see that $Z_T(\sqrt{\vec{k}^2 + m_g^2}, |\vec{k}|)$ is approximately equal to 1 for whole region of $|\vec{k}|$. Thus, we can approximate

$$\delta(\omega^2 \epsilon_T - \vec{k}^2) \approx \delta(\omega^2 - (\vec{k}^2 + m_g^2)). \quad (60)$$

Since longitudinal contribution is negligible, we can conclude that a gluon propagator in a hot dense medium can be approximated by

$$D_{\mu\nu} \approx -\frac{P_{\mu\nu}}{k^2 - m_g^2 + i\epsilon}. \quad (61)$$

References

- [1] Gyulassy M, Levai P, and Vitev I, Phys. Lett. B **538**, 282 (2002); Wang E and Wang X N, hep-ph/0202105; Salgado C A and Wiedemann U A, Phys. Rev. Lett. **89**, 092303 (2002); Gyulassy M, Vitev I and Wang X N, Phys. Rev. Lett. **86**, 2537 (2001).
- [2] Vitev I and Gyulassy M, Phys. Rev. Lett. **89**, 252301 (2002) [arXiv:hep-ph/0209161].
- [3] Zhakharov B G, JETP Lett. **63**, 952 (1996); Baier R *et al.*, Nucl. Phys. B **484**, 265 (1997); Wiedemann U A, Nucl. Phys. B **588**, 303 (2000).
- [4] Gyulassy M, Levai P, and Vitev I, Phys. Rev. Lett. **85**, 5535 (2000); Nucl. Phys. B **594**, 371 (2001); Phys. Rev. D **66**, 014005 (2002).
- [5] Gyulassy M, Wang X N, Nucl. Phys. B **420** (1994) 583; Wang X N, Gyulassy M, Plumer M, Phys. Rev. D **51** (1995) 3436
- [6] Wiedemann U A, Nucl. Phys. B **588** (2000) 303, Nucl. Phys. B **582** (2000) 409
- [7] Baier R, Dokshitzer Yu L, Mueller A H, Schiff D, Phys. Rev. C **58** (1998) 1706
- [8] Baier R, Schiff D, Zakharov B G, Ann. Rev. Nucl. Paer. Sci. **50** (2000) 37
- [9] Wang X N, Phys. Rev. Lett. **81** (1998) 2655, Phys. Rev. C **58** (1998) 2321

- [10] Gyulassy M and Plumer M, Nucl. Phys. A **527**, 641 (1991).
- [11] Gyulassy M, Plumer M, Thoma M and Wang X N, Nucl. Phys. A **538**, 37C (1992) ; Wang X and Gyulassy M, Phys. Rev. Lett. **68**, 1480 (1992).
- [12] Ter-Mikayelian M L, Dokl. Akad. Nauk SSSR **94** (1954) 1033
- [13] Ter-Mikayelian M L, High-Energy Electromagnetic Processes in Condensed Media, John Wiley & sons, New York (1972)
- [14] Djordjevic M, Gyulassy M, Phys. Lett. B **560** (2003) 37
- [15] Adcox K *et al.* [PHENIX Collaboration], Phys. Rev. Lett. **88**, 192303 (2002) [arXiv:nucl-ex/0202002].
- [16] Batsouli S, Kelly S, Gyulassy M, Nagle J L, Phys. Lett. B **557** (2003) 26
- [17] Adler C *et al.*, [PHENIX Collaboration] Phys. Rev. Lett. **89**, 202301 (2002).
- [18] S. S. Adler *et al.* [PHENIX Collaboration], arXiv:nucl-ex/0304022.
- [19] S. S. Adler *et al.* [PHENIX Collaboration], arXiv:nucl-ex/0306021.
- [20] (STAR Collaboration) C. Adler *et al.*, Phys. Rev. Lett. **89**, 202301 (2002) [arXiv:nucl-ex/0206011].
- [21] Adler C *et al.* [STAR Collaboration], arXiv:nucl-ex/0210033.
- [22] J. Adams *et al.* [STAR Collaboration], arXiv:nucl-ex/0305015.
- [23] B. B. Back *et al.* [PHOBOS Collaboration], arXiv:nucl-ex/0302015.
- [24] B. B. Back *et al.* (PHOBOS Collaboration), nucl-ex/0306025
- [25] I. Arsene *et al.*, (BRAHMS Collaboration), nucl-ex/0307003.
- [26] Gyulassy M, Vitev I, Wang X N and Zhang B W, arXiv:nucl-th/0302077;
- [27] A. Kovner and U. A. Wiedemann, arXiv:hep-ph/0304151; R. Baier, D. Schiff and B. G. Zakharov, Annu. Rev. Nucl. Part. Sci. **50**, 37 (2000)
- [28] Shuryak E V, Phys. Rev. C **55**, 961 (1997) [arXiv:nucl-th/9605011].
- [29] Mustafa M G, Pal D, Srivastava D K and Thoma M, Phys. Lett. B **428**, 234 (1998) [arXiv:nucl-th/9711059].
- [30] Lin Z W and Vogt R, Nucl. Phys. B **544**, 339 (1999) [arXiv:hep-ph/9808214]; Lin Z W, Vogt R and Wang X N, Phys. Rev. C **57**, 899 (1998) [arXiv:nucl-th/9705006].
- [31] Dokshitzer Y L and Kharzeev D E, Phys. Lett. B **519**, 199 (2001) [arXiv:hep-ph/0106202].
- [32] Kampfer B, Pavlenko O P, Phys. Lett. B **477** (2000) 171
- [33] Zakharov B G, JETP Lett. **76** (2002) 201
- [34] Biro T S, Levai P, Muller B, Phys. Rev. D **42** (1990) 3078

- [35] Peshier A, Kampf B, Pavlenko O P, Soff G, Phys. Rev. D **54** (1996) 2399
- [36] Levai P, Heinz U, Phys. Rev. C **57** (1998) 1879
- [37] Kalashnikov O K and Klimov V V, Sov. J. Nucl. Phys. **31**, 699 (1980).
- [38] Klimov V V, Sov. Phys. JETP **55** (1982) 199
- [39] Pisarski R D, PhysicaA **158** (1989) 146.
- [40] Rebhan A, Lect. Notes Phys. 583 (2002) 161, hep-ph/0105183; hep-ph/0111341.
- [41] Selikhov A V, Gyulassy M, Phys. Lett. B **316** (1993) 373; Phys. Rev. C **49** (1994) 1726.
- [42] Field R D, Applications of Perturbative QCD, Perseus Books, Cambridge, Massachusetts (1995)
- [43] Migdal A B, Phys. Rev. **103** (1956) 1811
- [44] Djordjevic M, Gyulassy M, Radiative heavy quark energy loss in QCD matter, to be published
- [45] Peskin M E, Schroeder D V, An Introduction to Quantum field Theory, Perseus Books, Cambridge, Massachusetts (1995)
- [46] Dokshitzer Y L, Khoze V A, Troian S I, Phys. Rev. D **53** (1996) 89
- [47] Kapusta J I, Finite-temperature field theory, Cambridge Monographs on Mathematical Physics (1993)
- [48] Le Bellac M, Thermal Field Theory, Cambridge Monographs on Mathematical Physics (2000)
- [49] Schoenmaker W J, Nucl. Phys. B **194** (1982) 535